Food Hydrocolloids 83 (2018) 355–364

Contents lists available at ScienceDirect

Food Hydrocolloids

journal homepage: www.elsevier.com/locate/foodhyd

Synthesis of monodisperse chitosan nanoparticles

David Joseph Sullivan [a, b], Malco Cruz-Romero [b], Timothy Collins [a], Enda Cummins [c], Joseph P. Kerry [b], Michael A. Morris [d, *]

[a] School of Chemistry, University College Cork, Cork, Ireland
[b] Food Packaging Group, School of Food & Nutritional Sciences, University College Cork, Cork, Ireland
[c] Biosystems Engineering, School of Agriculture, Food Science and Veterinary Medicine, Agriculture and Food Science Centre, University College Dublin, Belfield, Dublin 4, Ireland
[d] AMBER and the School of Chemistry, Trinity College Dublin, Dublin 2, Ireland

ARTICLE INFO

Article history:
Received 21 January 2018
Received in revised form
2 May 2018
Accepted 6 May 2018
Available online 8 May 2018

Keywords:
Synthesis of chitosan nanoparticles
Bottom-up and top-down
Monodispersity
Antimicrobial activity

ABSTRACT

The objectives of this study were to evaluate the effects of the initial concentrations of chitosan (CS) and sodium tripolyphosphate (TPP), the CS:TPP mass ratio, the CS molecular weight (MW) and pH on the synthesis of CS nanoparticles (CS NPs). The particle size of the synthesised CS NPs was significantly affected ($P < 0.05$) by these parameters. Self-assembled monodisperse CS NPs with a particle size of 90 nm and zeta potential of 30.15 mV were successfully synthesised using solutions of 0.1% low MW CS at pH 4.6 and 3:1 (CS:TPP) mass ratio. When higher concentrations of CS were used, application of external forces (tip sonication or Ultra-Turrax™) was necessary to induce monodispersity and significantly ($P < 0.05$) reduce the particle size; however, the particle sizes were >300 nm. While both native CS and CS NPs showed antimicrobial activity, no significant antimicrobial enhancement was observed for the NP form. The findings of this study have shown that monodisperse CS NPs can be obtained using a combination of bottom-up and top-down techniques and the unique physiochemical properties of these nanomaterials have the potential for applications in developing of antimicrobial active packaging materials.

1. Introduction

Numerous natural antimicrobials (NAMs) have been identified and applied in the food industry (Sullivan et al., 2018). However, of these NAMs, chitosan's (CS) numerous favourable properties such as GRAS status, biodegradability, biocompatibility and antimicrobial properties against a wide range of spoilage and pathogenic microorganisms along with its relative abundance and low cost have seen a significant increase in its applications in the food industry (Kong, Chen, Xing, & Park, 2010; Madureira, Pereira, Castro, & Pintado, 2015; Paomephan et al., 2018; Ryan et al., 2016). Structurally CS is made up of a random assortment of β(1–4)N-acetyl-D-glucosamine linkages where the ratio of the D-glucosamine to N-acetyl-D-glucosamine affects the physiochemical properties of bulk chitosan (Souza, Campiña, Sousa, Silva, & Gonçalves, 2013). While the antimicrobial mechanism of CS is not fully understood, several theories have been suggested that CS can either; electrostatically interact with negatively charged components of bacterial cell walls (Pilon et al., 2015) or through an ability to bind to DNA and inhibit RNA replication (Cruz-Romero, Murphy, Morris, Cummins, & Kerry, 2013). Moreover, studies have shown that the antimicrobial activity of CS is affected by intrinsic and extrinsic factors such as CS concentration, molecular weight (MW), degree of deacetylation (DD), pH and particle size (Antoniou et al., 2015; Kheiri, Moosawi Jorf, Malihipour, Saremi, & Nikkhah, 2016; Ngan et al., 2014).

Current research has been focused on the development of CS NPs for a wide range of applications in the food industry. CS NPs can be synthesised using either "bottom-up" or "top-down" techniques. Bottom-up is the self-assembly of atoms and molecules into larger nanoscale compounds (Sanguansri & Augustin, 2006), whereas a top-down approach is the breakdown of larger compounds into smaller nanoscale compounds through an external physical and/or chemical force (Ma, Liu, Si, & Liu, 2010). Studies have found that CS NPs can be developed through several different "bottom-up" approaches such as spray-freeze-drying which produce CS NPs (Gamboa et al., 2015), through reverse micelle medium methods

* Corresponding author.
E-mail address: morrism2@tcd.ie (M.A. Morris).

https://doi.org/10.1016/j.foodhyd.2018.05.010
0268-005X/

(Kafshgari, Khorram, Mansouri, Samimi, & Osfouri, 2012) or through the polymerisation of CS with methacrylic acid (PMAA) to make CS-PMAA NPs (de Moura, Aouada, & Mattoso, 2008). Top-down techniques have also been employed such as the wet milling process (Zhang, Zhang, & Xia, 2012) and high intensity ultrasound (Souza et al., 2013).

Currently the most widely used synthesis of CS NPs is through ionic gelation (Calvo, Remuñan-López, Vila-Jato, & Alonso, 1997), a bottom-up process whereby an anionic crosslinker such as sodium tripolyphosphate (TPP) is added to a solution of CS whereupon CS and TPP self-assemble into CS NPs. While many anionic crosslinkers such as glutaraldehyde (a toxic substance) can be used, TPPs favourable properties such as its biocompatibility and biodegradability make TPP a more suitable crosslinker for food applications. A facile top-down approach to particle size reduction is through the application of high intensity sonication techniques which reduce the overall particle size either through physical breakdown (cavitation mechanism) (Gokce, Cengiz, Yildiz, Calimli, & Aktas, 2014) or through free radical initiated polymer degradation (random schism model) (Wu, Zivanovic, Hayes, & Weiss, 2008).

Recent studies have reported increasing applications of CS NPs directly on food products and packaging materials as an antimicrobial in edible coatings (Pilon et al., 2015), against cheese microflora (O' Callaghan & Kerry, 2016), as a coating on Pacific whiteleg shrimp (Wang et al., 2015) and on red meats (Park, Marsh, & Dawson, 2010). Furthermore, due to CS NPs strong chelation ability they have been used as a carrier for both volatile antimicrobials such essential oils or extracts and polyphenols (Feyzioglu & Tornuk, 2016; Madureira et al., 2015) and in combination with metal ion nanoparticles such as silver and copper (Du, Niu, Xu, Xu, & Fan, 2009; Tran et al., 2010; Zain, Stapley, & Shama, 2014). These type of composite NPs have been applied to pork (Hu, Wang, Xiao, & Bi, 2015) and silver carp fillets (Zarei, Ramezani, Ein-Tavasoly, & Chadorbaf, 2015) among other foods.

Nonetheless, technical roadblocks for the application of CS NPs in the food industry exist including their economic cost and unknown toxicological effects. Regarding economic cost, bottom-up synthesis is preferential due to the facile and rapid production of sub 100 nm monodisperse CS NPs compared to top-down methods which have a limited particle size reduction and can also damage the structural properties of CS NPs (Ariga, Hill, & Ji, 2007). De Lima et al. (2010) evaluated the genotoxicity of CS-PMMA NPs using cytogenetic tests on human lymphocyte culture and the results indicated that CS-PMMA NPs over a particle size of 82 nm and a concentration of 180 mg L^{-1} were toxic to human lymphocyte cultures. Additionally, Wang, et al. (2016) investigated the embryonic toxicology of native CS and CS NPs on zebrafish (*Danio rerio*) where they observed that CS NPs with a particle size of 85 nm had less toxicity towards embryonic cells than native CS suggesting that CS NPs has lower toxicity compared to their bulk counterpart.

"Parameters such as initial CS or TPP concentration, CS:TPP mass ratio and pH at formation have individually or in combination been shown to affect the particle size and monodispersity of the synthesised CS NPs (Antoniou et al., 2015; de Pinho Neves et al., 2014; Fàbregas et al., 2013). However, to the best of our knowledge the combined effect of CS MW and pH of formation solution for the development of monodisperse CS NPs with a particle size <100 nm for applications in the food industry have not been studied. Therefore, the objectives of this study were to assess the effects of MW, pH, CS:TPP mass ratio and initial concentration of CS and TPP on the formation of monodisperse CS NPs using either bottom-up or top-down (tip sonication or Ultra-Turrax™) techniques. The synthesised nanomaterials were subsequently characterised and their antimicrobial activity assessed.

2. Materials and methods

2.1. Materials

Low molecular weight chitosan (L. MW) (MW; 50–190 kDa, ≥75% deacetylated), medium molecular weight chitosan (M. MW) (MW; 190–310 kDa, ≥75% deacetylated), aqueous acetic acid (HOAc), sodium hydroxide (NaOH) and sodium tripolyphosphate (TPP) were purchased from Sigma-Aldrich (St. Louis, MO, USA) and used as received. Mueller-Hinton Broth (MHB) and Maximum Recovery Diluent (MRD) were purchased from Oxoid (Basingstoke, UK). Reclaimed planar silicon [100] (p-type) substrates with a native oxide layer (2 nm) were used as received (Intel, Leixlip, Ireland). Cuvettes for zeta potential and particle size analysis were purchased from Malvern (Malvern Instruments Ltd, Malvern, UK).

2.2. Synthesis of chitosan nanoparticles

Bottom-up synthesis of CS NPs was carried out using ionic gelation method as previously described by Calvo et al. (1997) with some modifications. Briefly, different mass ratios of CS to TPP, molecular weight, pH and concentrations of both TPP and CS were assessed. Concentrations of 0.1% w/v low molecular weight (L. MW) and medium molecular weight (M. MW) CS were dissolved in 1% v/v acetic acid solution (pH 2.8) and in solution of pH 4.6 or 5.5 adjusted using 1 M NaOH, respectively. These solutions were then stirred at 600 rpm on a magnetic stirrer device (MSH-20D, Wise Stir, Korea) until clear homogenous solutions were formed and then left to stir for 1 h. Separately, 0.1 and 0.25% w/v solutions of TPP were prepared using sterile deionised water and stirred at 600 rpm for 1 h to ensure complete dissolution of TPP into solution. The TPP (0.1 or 0.25%) solution was added to the CS (L. MW or M. MW at pH 2.8, 4.6 or 5.5) solutions at a rate of 0.1 mL min^{-1} using a programmable peristaltic pump (Dose It P910, Integra Biosciences AG Switzerland) to a final mass ratio of CS:TPP of 3:1 under constant stirring at 800 rpm. When the concentration of CS was increased from 0.1 to 0.5% w/v; to reduce the overall average particle size external physical forces were used. These were an Ultra-Turrax™ DT-20 Tube with rotor-stator homogeniser at 4600 rpm for 1 min (IKA Werke, Janke & Kunkel GmbH & Co KG, Staufen, Germany) and tip sonication of CS NPs solutions in an ice bath using a 2 mm probe (EpiShear™ Probe Sonicator, Active Motif, UK) at 20 kHz frequency with an amplitude of 80% for 10 min in 30 s burst with 10 s rests.

2.3. Freeze-drying of chitosan nanoparticles

Fifteen mL of CS NPs solution were synthesised using 0.1% w/v L. MW CS at pH of 4.6 using a mass ratio 3:1. These parameters were chosen for freeze drying due to the product's small particle sizes and good monodispersity in order to get a direct weight to weight comparison of native CS to CS NPs for an MIC assay. The CS NP solution was poured into polystyrene petri dishes (Starsedt, Germany) and frozen at − 80 °C in a deep freezer (Sanyo, Japan) for 12 h before freeze-drying (Lyovac GT2, Steris, Hurth, Germany) under reduced pressure ($p < 0.1$ mbar) for 72 h. The freeze dried CS NPs were heat sealed in polyamide/polyethylene vacuum bags (Fispak, Dublin, Ireland) and stored at room temperature under darkness until required for FTIR and antimicrobial analysis.

2.4. Zetasizer particle characterisation

Particle size analysis, polydispersity index (PDI) and zeta potential measurements of CS and CS NPs were carried out using a Malvern Zetasizer Nano Series HT (Malvern, U.K.). CS NPs solutions (section 2.1) were loaded into a disposable cell (ZEN0040) and

analysis performed at 25 °C using a scattering angle of 173°. The material refractive index and viscosity of the 1% v/v acetic acid and water dispersant were defined as 1.333 and 0.890 cP, respectively and the material refractive index (CS NPs) set at 1.52 as previously determined using a handheld refractometer (OPTI, Bellingham + Stanley, Farnborough, U.K.). The particle size distribution and PDI was determined using the Mark–Houwink method while the zeta potential was determined using the Smoluchowski model. For the zeta potential analysis a disposable folded capillary tube (DTS1070) was filled with the CS or CS NPs solution and evaluated in automatic mode. Native CS and CS NPs solution were analysed in duplicate with 3 measurements per sample.

2.5. Scanning electron microscopy, atomic force microscopy and powder X-ray diffraction characterisation

Silicon wafer coupons (2 cm × 2 cm) were ultrasonicated (Cole-Palmer 8891, IL, USA) for 30 min twice in absolute ethanol. Solutions of native CS, 0.1 or 0.5% w/v CS NPs, prepared as outlined in section 2.2, were diluted (1:10) in absolute EtOH and ultrasonicated for 30 min. The homogenised diluted solutions of native CS or CS NPs solutions were spin coated (Specialty Coating Systems, 6800 spin coat series, IN, USA) onto the cleaned Si wafers at 3000 rpm for 30 s and dried under a stream of nitrogen (N_2) gas. Atomic Force Microscope (AFM, Park systems, XE-100, South Korea) imaging was carried out on the spin coated CS NPs Si wafers and scans performed in non-contact mode with high resolution, silicon microcantilever tips. Topographic images were recorded at a resonance frequency of 270–300 kHz. For the SEM imaging, CS NPs deposited on Si wafers were gold sputter coated by mounting loaded Si wafers onto an aluminium SEM stub with double sided carbon tape, and sputter coated with a 5 nm layer of gold/palladium (80:20) using a Quorum Q150 RES Sputter Coating System (Quorum Technologies, UK) and images of native CS and CS NPs spin coated on Si wafers were captured using a scanning electron microscope (SEM, FEI Company, FEG Quanta 6700). The SEM imaging was carried out at an accelerating voltage of 5 kV. Powder X-ray diffraction (PXRD) patterns of native CS and freeze-dried CS NPs were recorded on a Phillips Xpert PW3719 (Eindhoven, Netherlands) diffractometer using Cu Kα radiation. (Cu Kα, λ = 0.15418 nm, operation voltage 40 kV, current 40 mA).

2.6. FTIR analysis

Fourier transform infrared spectroscopy (FTIR) analysis of native CS, TPP and freeze-dried CS NPs was performed on a Varian 660-IR spectrometer (Varian Resolutions, Varian Inc, Victoria, Australia) using a diamond crystal ATR Golden Gate (Specac). Scans were taken with 32 scans at 2 cm^{-1} resolution in a wavenumber range from 4000 to 500 cm^{-1}.

2.7. Antimicrobial assay

2.7.1. Bacteria strains

In this study, antimicrobial activity of native L. MW and M. MW CS or freeze dried L. MW CS NPs against Gram-positive bacteria (*Staphylococcus aureus* (*S. aureus*) (NCIMB 13062) and *Bacillus cereus* (*B. cereus*) (NCIMB 9373)) and Gram-negative bacteria (*Escherichia coli* (*E. coli*) (NCIMB 11943) and *Pseudomonas fluorescens* (*P. fluorescens*) (NCIMB 9046)) were assessed. Before use, all pure culture bacteria were grown for 18 h at 30 °C (*P. fluorescens and B. cereus*) or 37 °C (*S. aureus* and *E. coli*) in Mueller-Hinton broth (MHB) (Oxoid, UK) under constant agitation at 170 rpm on an orbital shaker (Innova 2300, New Brunswick™, Germany).

2.7.2. Antimicrobial activity test

The antimicrobial activity of native CS or freeze dried CS NPs dissolved in 1% v/v acetic acid solution and pH adjusted to 4.6 were measured by determining the minimum inhibitory concentration (MIC) against the target microorganisms in a 96 flat bottom well tissue culture microplates (Sarstedt Inc., NC, USA) according to the NCCLS (2000) broth microdilution method as described by Cruz-Romero et al. (2013). Bacterial strains were cultured overnight at the appropriate temperature as outlined in section 2.8.1 and adjusted to a final density of 10^5 CFU mL^{-1} using maximum recovery diluent and used as an inoculum within 15 min of preparation. Briefly, 100 μL of double-strength MHB (2XMHB) was added to each well in rows A to F, 200 μL of adjusted bacterial culture suspension was added to row H in columns 1–11 and 200 μL of sterile 2XMHB was added to column 12. In each well of row G, 200 μL of 0.1% w/v native CS or CS NP solutions were dispensed and a twofold serial dilution was performed by transferring 100 μL of antimicrobial solutions from row G into the corresponding wells of row F through to row B. After mixing, 100 μL of the resultant mixture on row B was discarded. Finally, using a 12-channel electronic pipette (Model EDP3-Plus, Rainin, USA) 15 μL of the tested microorganisms was pipetted from each well in row H into the corresponding wells in row A followed by rows B to G. Positive (Row A) and negative growth controls (Column 12) were included in each assay plate. The inoculated plates were incubated in a wet chamber for 24 h at 30 °C (*P. fluorescens* and *B. cereus*) or 37 °C (*E. coli* and *S. aureus*). The lowest concentration showing inhibition of growth was considered to be the MIC for the target microorganisms. The test was repeated in duplicate in two independent experiments.

2.8. Statistical analysis

Statistical analysis was performed using the software STATGRAPHICS® centurion XV (Statpoint, Inc., USA). To assess the effects of pH and MW on the particle size, PDI, zeta potential and MIC a two-way analysis of variance (ANOVA) was carried out. Interaction between factors, treatment means and least significant difference (LSD) values are presented ($P < 0.05$). To assess the effects of chitosan to TPP mass ratio, the effects of physical treatments of CS NPs and dissolution pH of freeze dried CS NPs on the particle size distribution, zeta potential, and polydispersity index, a one-way ANOVA was used. A difference between pairs of means was resolved by means of confidence intervals using Tukey's test. The level of significance was set at $P < 0.05$.

3. Results and discussion

3.1. Effect of TPP concentration, mass ratio, pH and molecular weight on the formation of monodisperse self-assembled chitosan nanoparticles

The effects of the initial pH and MW of CS on the average particle diameter, polydispersity index (PDI) and zeta potential of CS NPs are shown in Table 1. Both parameters significantly ($P < 0.05$) affected the particle size, PDI and zeta potential of the synthesised CS NPs. Overall L. MW CS produced smaller average particle size compared to M. MW CS. These results are in agreement with the findings of O'Callaghan and Kerry (2016) who reported that the particle size of CS NPs was significantly affected by the MW of CS. However, the relatively small increase in particle size observed between L.MW CS and M.MW CS at pH 4.6 is from the conformation of CS in solution as L. MW CS has an extended rod conformation whereas M. MW has a random coil conformation (Qun & Ajun, 2006). Results of the PDI, a dimensionless measure of the range

Table 1
Effects of pH and chitosan molecular weight on the Particle size distribution, polydispersity index and zeta potential during synthesis of chitosan nanoparticle*.

	Particle size distribution (nm)	PDI	Zeta potential (mV)
A: MW			
L.MW	120.057[a]	0.266a	29.46[a]
M.MW	186.006[b]	0.481[b]	26.21[b]
SL	0.000	0.000	0.00
B: pH			
pH2.8	224.042[a]	0.679[a]	44.14[a]
pH4.6	104.793[b]	0.235[b]	25.96[b]
pH5.5	130.258[c]	0.207[c]	13.39[c]
SL	0.000	0.000	0.00
Interaction (A × B)			
L.MW,pH2.8	143.07 ± 2.46[a]	0.462 ± 0.007[a]	42.28 ± 186[a]
L.MW,pH4.6	92.92 ± 6.69[b]	0.155 ± 0.038[b]	30.15 ± 2.45[b]
L.MW,pH5.5	120.58 ± 10.82[c]	0.173 ± 0.017[c]	15.93 ± 1.20[c]
M.MW,pH2.8	305.02 ± 27.82[d]	0.896 ± 0.036[d]	46.00 ± 1.52[d]
M.MW,pH4.6	113.07 ± 8.09[e]	0.307 ± 0.067[e]	21.80 ± 1.98[e]
M.MW,pH5.5	139.93 ± 9.09[f]	0.242 ± 0.049[f]	10.84 ± 0.77[f]
LSD	3.122	0.0096	0.405

*All values are means of triplicate measurements from two independent experiments (n = 6).
[a,b,c,d,e,f] different subscripts in the same column indicate significant differences ($P < 0.05$). SL = significance level.

of the particle size distribution calculated from the cumulant analysis, indicated that MW significantly ($P < 0.05$) affected PDI of CS NPs where L. MW CS had lower PDI compared to M. MW CS. MW was also shown to have an effect on zeta potential where L. MW CS NPs had a larger overall zeta potential compared to M. MW CS NPs. Regarding the effects of pH on the synthesis of CS NPs, the smallest CS NPs particle size was obtained when CS NPs were synthesised at pH 4.6 while CS NPs synthesised at pH 2.8 gave the largest particle size. These results are in agreement with other studies which have observed that CS NP formed above or below a critical pH range of 4.5–5.2 will have larger average particle sizes (Fan, Yan, Xu, & Ni, 2012; Gokce et al., 2014). The effect of pH on the particle size of CS NPs is believed to be due to the degree of protonation of the CS amine group. At pH 4.6, more protonation of the CS amine occurs which allows for greater interaction with anionic TPP ions, resulting in smaller CS NPs. However, CS NPs synthesised using pH 2.8 showed larger particle diameter and may perhaps be due to the increased ionic strength of CH_3CHOO^- anions shielding the interaction of protonated CS amine groups with anionic TPP, therefore, reducing the number of crosslinking sites and resulting in larger CS NPs (Fan et al., 2012). At pH 5.5, CS amine is less protonated and consequently more anionic TPP has to interact with the CS polymer to stabilise the CS NPs and so resulting in larger CS NPs (Mi, Shyu, Lee & Wong, 1999). With respect to PDI, CS NPs at pH 5.5 had the lowest PDI while NPs synthesised using pH 2.8 had the largest PDI. The pH was also shown to affect the zeta potential of CS NPs as the zeta potential at pH 2.8 was the largest measured zeta potential whereas the lowest was measured at pH 5.5. This may be linked to the degree of protonation of the CS NPs solution.

The interactive effect of MW and pH was also shown to have a significant ($P < 0.05$) effect on the particle size distribution, PDI and zeta potential of the synthesised CS NPs. The lowest particle size and PDI was observed when CS NPs were synthesised using L. MW CS at pH 4.6 (92 nm) and the largest CS NPs particle size and PDI was observed using M. MW CS at pH 2.8. Furthermore, zeta potential measurements show that L. MW and M. MW CS NPs synthesised at pH 2.8 had the largest zeta potentials (Table 1). Additionally, the zeta potential of L. MW CS NPs at pH 4.6 was recorded to be also above the ±30 mV threshold and are considered as moderately stable colloids and are therefore, less susceptible to agglomeration and destabilisation forces such as van der Waals forces, Brownian motion or particle – particle interactions (Gokce et al., 2014; Mohanraj and C., 2006).

Since L. MW CS at pH 4.6 gave CS NPs with the smallest average particle diameter and more stable colloids (due to the higher zeta potential), the effect of TPP concentration and mass ratio of CS:TPP on the synthesis of CS NPs was investigated using this reaction condition. Initially, the TPP concentration was increased from 0.1 to 0.25% w/v maintaining a constant mass ratio of CS:TPP where the particle size analysis indicated that the initial concentration of TPP significantly ($P < 0.05$) affected the particle size of the formed CS NPs, with greater particle size and higher PDI obtained in CS NPs synthesised using 0.25% w/v TPP (Table 2). These results are in agreement with the findings of Fan et al. (2012) who reported that the reduction of TPP concentration corresponded to a reduction in the overall particle size distribution of CS NPs; whereas higher concentrations of TPP result in larger, polydisperse CS NPs (Qi, Xu, Jiang, Hu, & Zou, 2004). The use of concentrations of 0.1% w/v TPP yielded smaller NPs due to the smaller number of counter ionic sites of TPP interacted with CS; reducing the potential for an excess net negative charge from the TPP needing to be balanced with more cationic CS, which can result in the agglomeration of CS NPs. The CS:TPP mass ratio affected the formation of CS NPs in a complex manner. The 6:1, 3:1 and 1:1 CS:TPP mass ratios (maintaining a constant CS concentration of 0.1% w/v (Table 2)) indicated that the most stable CS:TPP mass ratio for the formation of CS NPs was 3:1 since CS NPs formed using this mass ratio had the smallest average particle diameter (90.5 nm) and PDI (0.164) while having the highest zeta potential (30.15 mV). This represents the basic CS NP colloid unit and when parameters (such as mass ratio or concentration) are changed, aggregation of CS NPs into larger agglomerates occurs.

Comparatively, mass ratios of 6:1 and 1:1 showed significantly ($P < 0.05$) larger PDI values and lower zeta potential measurement (Table 2) while 1:1 samples also had significantly ($P < 0.05$) larger particle size distribution than 3:1 and 6:1 samples. A study carried out by Antoniou et al. (2015) used concentrations of 0.5 mg mL^{-1} L. MW CS and 0.7 mg mL^{-1} TPP in different mass ratios to synthesise CS NPs and found that the CS NPs particle size distribution decreased when the mass ratio CS:TPP up to 9:1 was used; however, when larger concentration of CS than 9:1 mass ratios were used, larger CS NPs were formed. In this study, CS NP solutions made using a mass ratio of 6:1 were transparent while solutions made using a 3:1 mass ratio were slightly opaque; however, solutions with a mass ratio of 1:1 were turbid and large agglomerates were observed (Fig. 1). Since CS NPs are polymers, their nucleation

Table 2
Effects of chitosan to TPP mass ratio on the particle size distribution, polydispersity index and zeta potential at formation of CS NP*.

	Particle size distribution (nm)	PDI	Zeta potential (mV)
0.1% w/v L. MW CS NPs (6:1)	100.17 ± 0.89^{a}	0.264 ± 0.016^{a}	20.48 ± 1.68^{a}
0.1% w/v L. MW CS NPs (3:1)	96.52 ± 2.83^{a}	$0.195 \pm 0.013^{a,b}$	30.15 ± 2.45^{b}
0.1% w/v L. MW CS NPs (1:1)	20206.67 ± 4651.12^{b}	0.458 ± 0.287^{b}	9.81 ± 1.43^{c}

*All values are means of triplicate measurements from two independent experiments (n = 6).
[a,b,c,] Mean values in the same row with different superscripts are significantly different ($P < 0.05$).

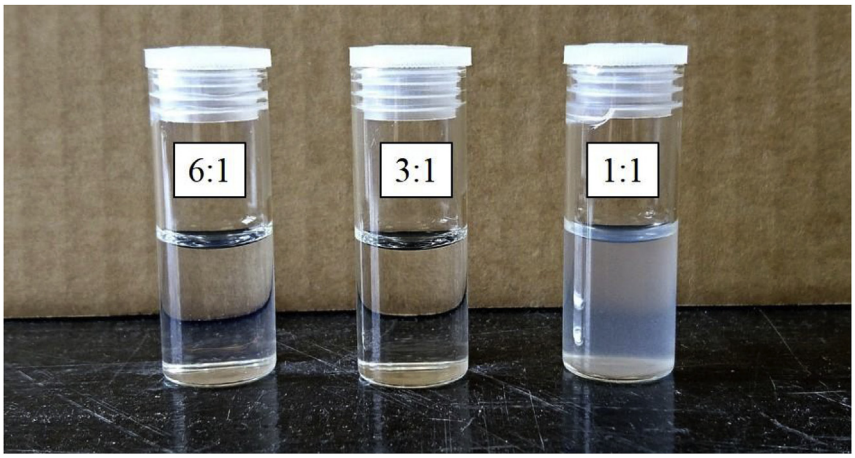

Fig. 1. Visual Image of chitosan nanoparticles at pH 4.6 in 6:1, 3:1 and 1:1 CS:TPP mass ratios (from left to right) where 1:1 is the most turbid while 3:1 is least turbid.

mechanism of formation will differ if compared to metallic ion nanoparticles. Rathi and Gaikar (2017) reported that higher CS concentration leads to the generation of many nuclei; however, these nuclei have higher growth rates due to repulsion between the CS chains and result in the formation of bigger CS NPs.

To assess the effects of initial CS concentration at formation of CS NPs at pH 4.6; initial concentration of L. MW CS was increased from 0.1 to 0.5% w/v (Table 3). Results showed that the increase of the initial concentration significantly increased ($P < 0.05$) the average particle diameter of CS NPs from 90.5 nm to 1687.167 nm before physical treatments and increased the PDI of CS NPs from 0.195 to 0.662 (Table 3). Therefore, size reduction techniques such as tip sonication and an Ultra-Turrax™ DT-20 were employed to reduce the particle size of the agglomerated CS NPs. While both treatments showed a significant ($P < 0.05$) reduction in the average particle size and PDI compared to untreated CS NPs, size reduction was more efficient ($P < 0.05$) when tip sonication was used compared to Ultra-Turrax™ DT-20 Tube (Table 3); however, Ultra-Turrax™ DT-20 treatment showed a significant increase in the zeta potential compared to untreated and tip sonicated CS NPs. Previous studies have reported that tip sonication treatment is more effective at size reduction of CS NPs due to its mechanism of particle breakdown and is through a cavitation mechanism whereby acoustic energy generated by the sonicator creates rapidly collapsing bubbles thus creating a transient high pressure gradient and high velocity within the liquid which subsequently creates a shear force that can break the CS polymer chain at the β(1–4) linkage, due to the difference in bond energy between the two moieties (Wu et al., 2008). Furthermore, other breakdown mechanism such as hydrolysis or fragmentation mechanisms have also been reported (Renata Czechowska-Biskup et al., 2005). Moreover, tip sonication is also advantageous as its particle size reduction mechanisms precludes CS NPs below a certain particle size, reducing potential damage to their structure and targeting larger CS NPs for size reduction (Antoniou et al., 2015).

When freeze-dried (0.1% w/v) CS NPs were dispersed in water or 1% v/v HOAc (pH 2.8) or pH 4.6 (adjusted using 1 M NaOH) and tip sonicated to deagglomerate CS NPs into the solution; the largest particle size was observed when CS NPs were dispersed in water (1288 nm) while the smallest average particle diameter was observed when CS NPs were dispersed in 1% HOAc at pH 4.6 solution (318 nm). Similarly, the smallest PDI value was recorded for CS NPs at pH 4.6 whereas CS NPs dispersed in pH 2.8 and 7 had larger PDI values. The results indicated that freeze-dried CS NPs were significantly larger than CS NPs synthesised in situ: however, the zeta potential followed a similar trend that linearly increased when pH decreased (Table 4).

Table 3
Effect of physical treatments on the particle size distribution, zeta potential, and polydispersity index of CS NPs*.

	Particle size distribution (nm)	PDI	Zeta potential (mV)
0.5% w/v CS NPs untreated	1687.167 ± 412.27^{a}	0.662 ± 0.114^{a}	31.32 ± 3.49^{a}
0.5% w/v CS NPs Ultra-Turrax™	1130.83 ± 98.01^{b}	0.446 ± 0.157^{b}	44.75 ± 2.76^{b}
0.5% w/v CS NPs Tip sonication	385.13 ± 10.44^{c}	0.303 ± 0.034^{c}	32.35 ± 3.79^{a}

*All values are means of triplicate measurements from two independent experiments (n = 6).
[a,b,c,] Mean values in the same row with different superscripts are significantly different ($P < 0.05$).

Table 4
Effect of tip sonication treatment on the particle size distribution, polydispersity index and zeta potential of freeze-dried CS NPs dissolved at different pH *.

	Particle Size Distribution (nm)	PDI	Zeta Potential (mV)
0.1% w/v CS NPs (Freeze-dried, pH 7)	1287.92 ± 424.55^{a}	0.855 ± 0.109^{a}	13.07 ± 12.87^{a}
0.1% w/v CS NPs (Freeze-dried, pH 4.6)	317.55 ± 71.08^{b}	0.350 ± 0.045^{b}	22.68 ± 1.79^{b}
0.1% w/v CS NPs (Freeze-dried, pH 3)	677.27 ± 109.08^{c}	$0.693 \pm 0.05)2^{c}$	39.73 ± 0.98^{c}

*All values are means of triplicate measurements from two independent experiments (n = 6).
[a,b,c,] Mean values in the same row with different superscripts are significantly different ($P < 0.05$).

3.2. Morphological and topographical analysis of CS NPs

The morphological features of native L. MW CS and CS NPs synthesised using bottom-up and top-down techniques are shown in Fig. 2 while topographical features of 0.1 and 0.5% w/v L. MW CS NPs made using L. MW CS at pH 4.6 are shown in Fig. 3. Native L. MW CS at an initial concentration of 0.1% w/v has semi-crystalline nature with a fibril and irregular morphology and a wide particle size distribution (Fig. 2a). CS NPs synthesised through a bottom-up self-assembly process using an initial concentration of 0.1 w/v% L. MW CS at pH 4.6 using a 3:1 CS to 0.1% w/v TPP mass ratio had a regular spherical morphology and a monodisperse particle size distribution typical of rapid solution processing (Fig. 2b). However, when the initial concentration of CS was increased to 0.5% w/v agglomeration of CS NPs was observed (Fig. 2c). Therefore, tip sonication was applied to CS NPs and resulted in NP with rod-like morphologies and a significant particle size reduction and an increase in monodispersity (Fig. 2d). Furthermore, CS NPs synthesised using 0.5% w/v CS also showed larger average particle diameter compared to NPs synthesised using 0.1% w/v CS. For AFM analysis, due to the irregular and large size features of native CS, topographical imaging was carried out only on 0.1 and 0.5% w/v CS NPs and the results showed that the average particle diameter of CS NPs were 26.59 and 34.18 nm, respectively (Fig. 3). The particle size obtained using AFM analysis was up to 70.6 or 92.2% smaller for 0.1 and 0.5% w/v CS NPs, respectively than the results obtained by the Zetasizer. Due to the hygroscopic nature of the CS NPs, apparently the drying effect of absolute EtOH used as dispersant of the CS NPs significantly ($P < 0.05$) reduced overall particle size obtained using the AFM compared to the particle size obtained using the hydrodynamic analysis technique. This results suggests that CS NPs are extremely swollen in aqueous solution and have good absorption ability which can be used to enhance the antimicrobial activity of the CS NPs as studies have showed that the incorporation of other NAMs such as essential oils or non-NAMs such as silver nanoparticles, can increase the antimicrobial activity of CS NPs (Hosseini, Rezaei, Zandi, & Farahmandghavi, 2016; Zain et al., 2014). PXRD analysis of native CS (powder form) and freeze-dried CS NPs revealed the semi-crystalline nature of native CS. Typical PXRD diffractograms showed a low intensity peak at 20.13° and this results are in agreement with results reported by Shahbazi, Rajabzadeh, and Ahmadi (2017). However, the PXRD analysis of CS NPs did not show a distinct peak indicating the amorphous nature of CS NPs which was attributed to the crosslinking between CS & TPP which prevents alignment of the chitosan chains (see supplemental material) (Qi et al., 2004).

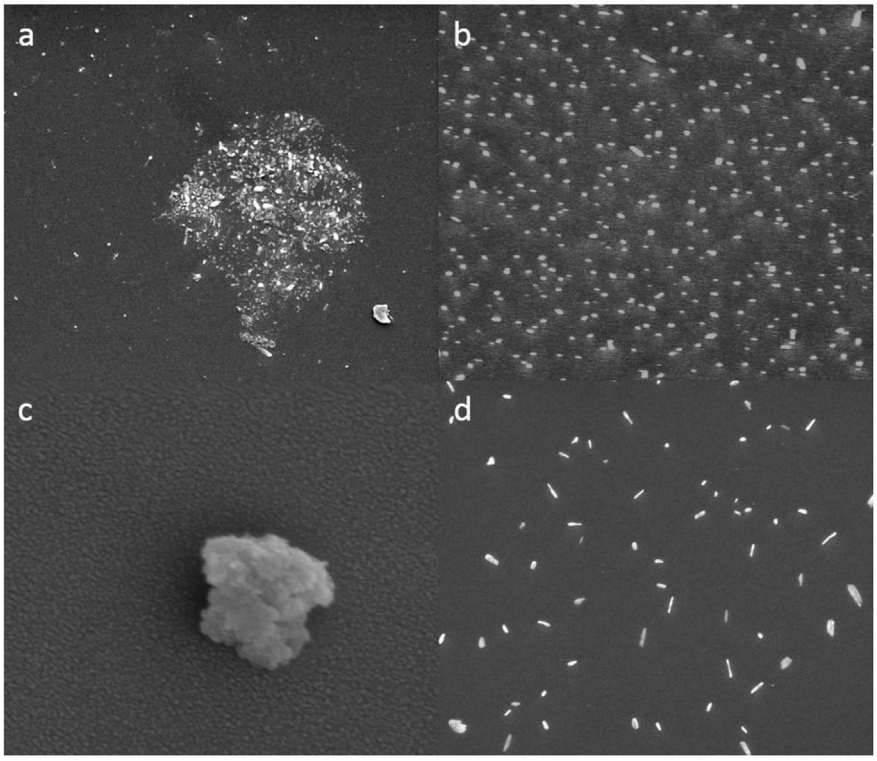

Fig. 2. SEM micrograph of native low molecular weight chitosan (a), 0.1% w/v chitosan nanoparticles (b), untreated 0.5% w/v chitosan nanoparticles (c) and tip sonicated treated 0.5% w/v chitosan nanoparticles.

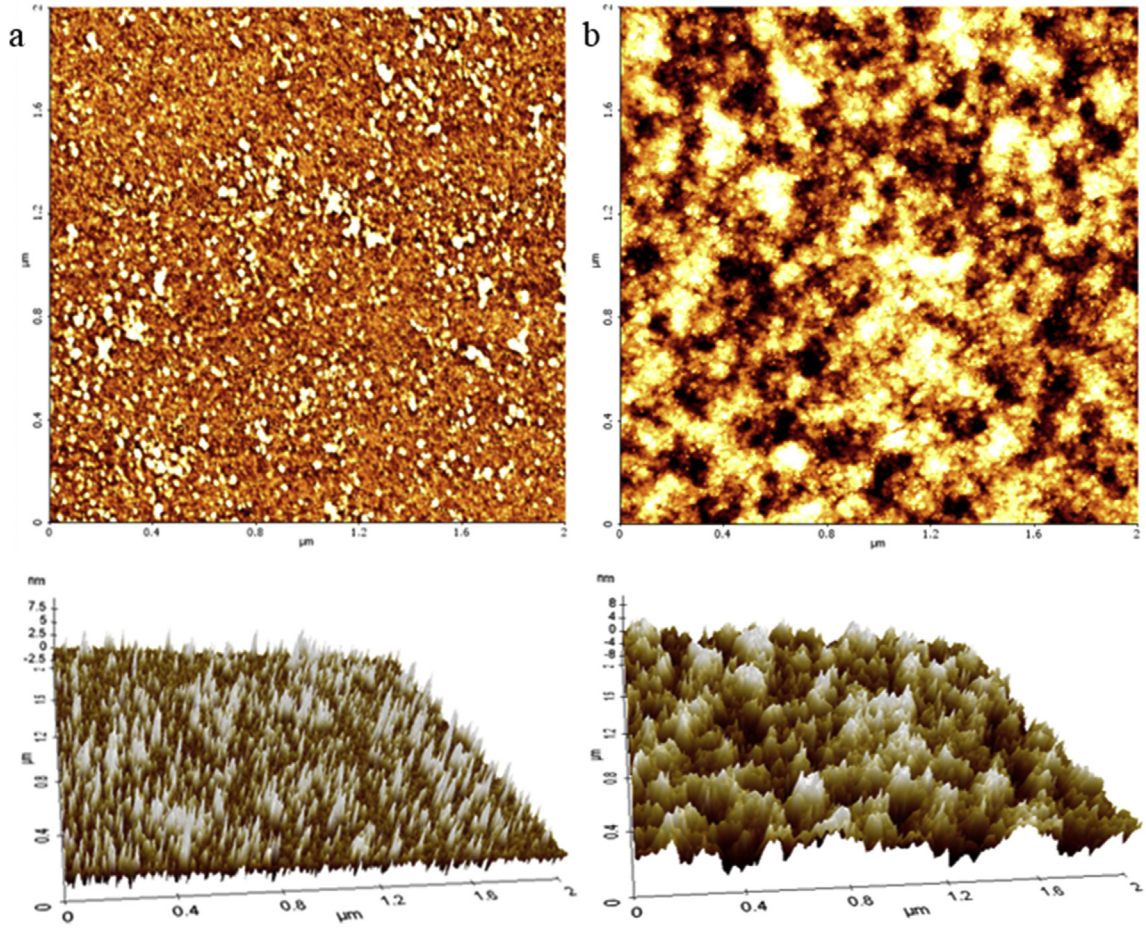

Fig. 3. AFM images of 0.1 (a) and 0.5 (b) w/v% chitosan nanoparticles showing both 2D and 3D topographical images.

3.3. FTIR analysis

The FTIR spectrum of native L. MW CS, TPP and freeze dried L. MW CS NPs are shown in Fig. 4. The FTIR spectra of native L. MW CS showed major peaks at; 1027 cm^{-1} indicating a C – O – C symmetric stretch (from the glucosamine unit of CS), 1542 cm^{-1} which suggests an aromatic C – C bonds, 1650 cm^{-1} indicated a bending primary amine, 2865 cm^{-1} suggests a C – H vibrational stretching band and the broad peak from 3200 to 3500 cm^{-1} is a combination of symmetric and asymmetric – NH_2 and vibrational – OH stretches and these results are in agreement the result reported by de Pinho Neves et al. (2014). The CS NP spectra differed from the native CS where several peaks such as the aromatic C – C which shifted from 1585 cm^{-1} to 1542 cm^{-1} and the primary amine at 1650 cm^{-1} shifted to 1633 cm^{-1} while the broad overlapping N – H and O – H peak at 3200–3400 cm^{-1} has decreased peak intensity and definition suggesting that ionic gelation occurred between the protonated amine and the counter anion present in TPP. However, the C – O – C peak at 1027 cm^{-1} and the C – H peak at 2865 cm^{-1} remained unaffected and this results are in agreement with the results reported by Antoniou et al. (2015) and de Pinho Neves et al. (2014). The FTIR spectra of TPP powder showed peaks at 875 cm^{-1} corresponding to both O – P – O and P – O stretches and a peak at 1126 cm^{-1} which corresponded to a P = O stretch. The peak intensity at those wavelengths were lower in the CS NP spectra and this results are similar to the reported by Antoniou et al. (2015).

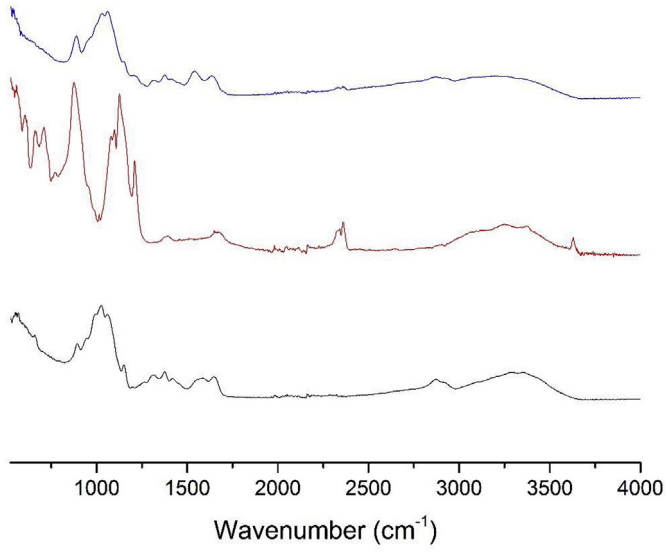

Fig. 4. FTIR spectra of chitosan (—), sodium tripolyphosphate (—) and chitosan nanoparticles (—).

3.4. Antimicrobial activity of CS NPs

Antimicrobial activity of L. MW and M. MW CS at pH 2.8, pH 4.6 or pH 5.5, respectively and freeze-dried CS NPs synthesised at pH 4.6 using a mass ratio of 3:1 CS:TPP against Gram-positive (*S. aureus*

and *B. cereus*) and Gram-negative (*E. coli* and *P. fluorescens*) bacteria (common food spoilage microorganisms) indicated that the pH and MW of native CS significantly ($P < 0.05$) affected the antimicrobial efficacy (Fig. 5). Independent of pH, L. MW CS was observed to have greater antimicrobial activity against *S. aureus*, *B. cereus* and *P. fluorescens*; however, *E. coli* was shown to be more susceptible to M. MW CS. Studies in the literature have widely reported that L. MW CS has better antimicrobial activity, due its ability to penetrate the cell wall of microbes and combine with their DNA, thus inhibiting the synthesis of mRNA and DNA transcription (Cruz-Romero et al., 2013; Liu et al., 2006). However, other authors have reported that M. MW CS is more effective as it can form a film that encapsulates bacteria, inhibiting nutrient uptake (Chang, Lin, Wu, & Tsai, 2015). This suggests that the primary mechanism of antimicrobial activity of CS differed between bacterial strains. Independent of MW, pH was shown to have a significant effect on the antimicrobial activity. CS at pH 2.8 was the most effective antimicrobial while CS at pH 5.5 had the least effective antimicrobial activity. Herein it has been shown that lower pH (2.8) increased the antimicrobial activity. Similarly, previous studies have found that significantly higher antimicrobial activity of CS occurs at lower pH compared to a higher pH as a result of increased CS amine group protonation in acidic solutions (Kong et al., 2010; Rabea, Badawy, Stevens, Smagghe, & Steurbaut, 2003). Overall it was observed that the greatest antimicrobial activity of native CS was L. MW CS at pH 2.8, while the least antimicrobial effectiveness was observed using L. MW or M. MW CS at pH 5.5.

The antimicrobial activity of the synthesised CS NPs indicated that *E. coli* and *B. cereus* were less susceptible to the CS NPs than *P. fluorescens* and *S. aureus* (Fig.5). Herein it was observed that the MIC of CS NPs against *P. fluorescens* and *S. aureus* was 0.125 mg mL^{-1} while a concentration of 0.25 mg mL^{-1} was needed to inhibit *E. coli* and *B. cereus*. Comparatively, MICs values obtained in this study are lower than the MIC against *S. aureus, B. cereus, P. fluorescens* and *E. coli* reported by O'Callaghan and Kerry (2016) who found the most susceptible bacteria to CS NPs was *P. fluorescens* (0.22 mg mL^{-1}) while the least susceptible bacteria was *S. aureus* (0.28 mg mL^{-1}). In this study, CS NPs did not show enhanced antimicrobial activity when compared to native CS. Our results are in agreement with the findings of Ristić, Lasič, Kosalec, Bračič, and Fras-Zemljič (2015) who reported that CS had greater antimicrobial activity than CS NPs due to the cationic amines being taken by the ionic gelation and resulted in less protonated amines available for interaction with negatively charged components of bacterial cells. This may also be due to the strong solvent swelling character of CS NPs, as when in aqueous solution the particle size of CS NPs will increase and this may perhaps reduce the potential ability to interact with bacterial cell component reducing the antimicrobial activity of the CS NPs. Furthermore, when CS and CS NPs were compared on a percent weight by weight basis (% w/w), the concentration of CS in CS NPs was lower due to a different structural composition of CS NPs and native CS as CS NPs have in their structure antimicrobial CS and TPP as they were synthesised using a 3:1 (CS:TPP) mass ratio which may decrease the antimicrobial activity of CS NPs if compared to a similar weight of native CS. In addition the different structural composition of CS NPs may perhaps explain the reduced toxicity of CS NPs as Wang et al. (2016) found that CS NPs were less toxic than native CS and as reported herein native CS and CS NPs have the similar antimicrobial activity which may apparently make the application of CS NPs in food more favourable compared to CS. Nevertheless, studies have reported that CS NPs showed enhanced antimicrobial properties compared to their non-nano equivalents (Ngan et al., 2014; Qi et al., 2004). Enhanced antimicrobial activity of CS NPs was attributed to the

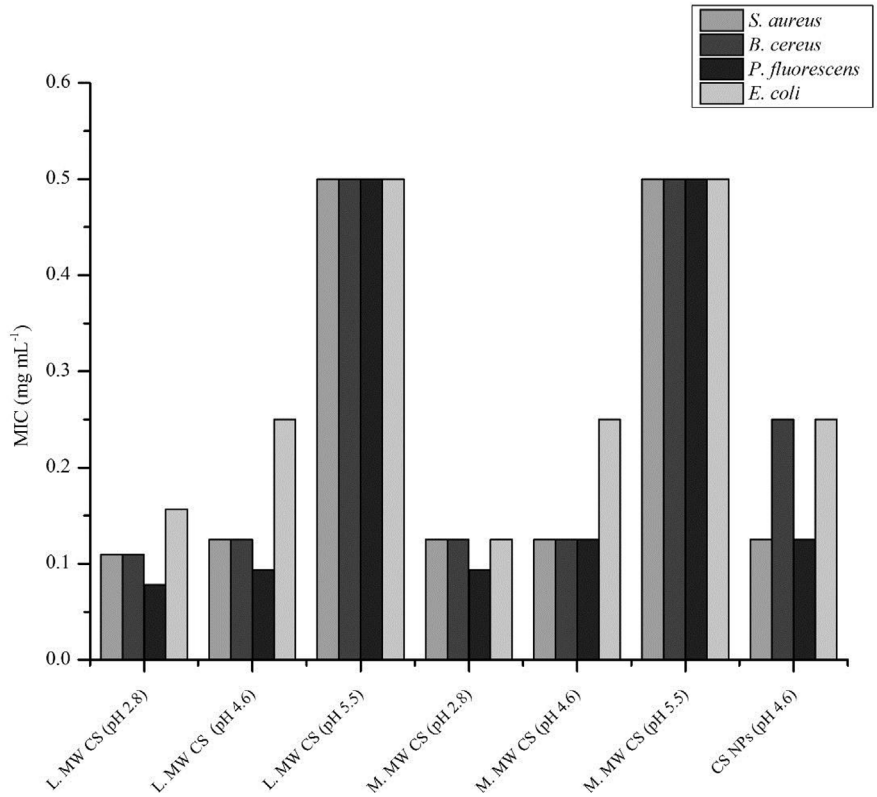

Fig. 5. Effects of pH (2.8, 4.6 or 5.5) or molecular weight (low or medium molecular weight) of chitosan and low molecular weight chitosan nanoparticles at pH 4.6 on the antimicrobial activity (Minimum inhibition concentration (mg mL^{-1})).

increased surface area compared to their bulk counterpart thus allowing more interaction with the bacterial cell components (Maillard & Hartemann, 2013).

Additionally, it has been reported that the antimicrobial activity of native CS is not only affected by pH and MW but also by other intrinsic and extrinsic factors such as degree of deacetylation (DD) of CS and bacterial type (e.g. Gram stain). The effects of the DD on the antimicrobial activity of CS were reported to be due to the greater number of amine groups that can be protonated (Li, Wu, & Zhao, 2016). In general an increased DD was reported to have an increased antimicrobial activity; however, when DD > 85%, antimicrobial efficacy of CS does not significantly increase (Li et al., 2016). The Gram strain of the bacteria has also been reported to affect CS antimicrobial efficacy. Herein, within the Gram-negative bacteria tested *P. fluorescens* was the most susceptible to native CS compared to *E. coli*. Concerning Gram-positive bacteria, it was found that *B. cereus* was more susceptible to native CS than *S. aureus*. It has been reported that Gram-negative bacteria such as *Pseudomonas* spp. are more susceptible due to polycationic CS that can compete with stabilising divalent metals (e.g. Mg^{2+}, Ca^{2+}) in the cell wall of Gram-negative bacteria leading to structural destabilisation (Cruz-Romero et al., 2013). However, other studies have reported that CS is more antimicrobially active against Gram-positive bacteria such as *S. aureus* due to CS ability to form linkages with lipoteichoic acid on the cell surface of Gram-positive bacteria, disrupting membrane functions (Goy, Morais, & Assis, 2016). Regarding CS NPs, Gram-positive bacteria such as *B. cereus* may show less susceptibility owing to the positive zeta potential of CS NPs hindering interaction with bacterial cells (Simon-Deckers et al., 2009).

4. Conclusion

Factors such as MW, pH, CS and TPP concentration and CS:TPP mass ratio significantly affected ($P < 0.05$) the particle size of the synthesised CS NPs. The interactive effect of MW and pH on the formation of CS NPs showed that optimal particle size was obtained when L. MW CS at a pH of 4.6 was used. The parameters to synthesise monodisperse CS NPs using the bottom-up technique with an average particle size of 90 nm and zeta potential of 30.15 mV were 0.1% w/v L. MW CS at pH 4.6 and 3:1 (CS:TPP) mass ratio. When higher initial concentrations of CS were used, the application of external forces such as tip sonication was required to induce monodispersity and reduce the particle size; however, the particle size was >300 nm. In native CS the initial pH significantly affected ($P < 0.05$) the antimicrobial activity where pH 2.8 showed greater antimicrobial efficacy compared to CS solutions at pH 4.6 and 5.5. While antimicrobial activity of CS NPs was not significantly higher than native CS; however, monodisperse CS NPs unique physiochemical properties may find applications in the development of antimicrobial active packaging.

Acknowledgements

This work was funded under the National Development, through the Food Institutional Research Measure (FIRM) administered by the Department of Agriculture, Food and the Marine, Republic of Ireland (11/F/038).

Appendix A. Supplementary data

Supplementary data related to this article can be found at https://doi.org/10.1016/j.foodhyd.2018.05.010.

References

Antoniou, J., Liu, F., Majeed, H., Qi, J., Yokoyama, W., & Zhong, F. (2015). Physicochemical and morphological properties of size-controlled chitosan–tripolyphosphate nanoparticles. *Colloids and Surfaces a: Physicochemical and Engineering Aspects, 465*, 137–146.

Ariga, K., Hill, J. P., & Ji, Q. (2007). Layer-by-layer assembly as a versatile bottom-up nanofabrication technique for exploratory research and realistic application. *Physical Chemistry Chemical Physics, 9*(19), 2319–2340.

Calvo, P., Remuñan-López, C., Vila-Jato, J. L., & Alonso, M. J. (1997). Chitosan and chitosan/ethylene oxide-propylene oxide block copolymer nanoparticles as novel carriers for proteins and vaccines. *Pharmaceutical Research, 14*(10), 1431–1436.

Chang, S. H., Lin, H. T., Wu, G. J., & Tsai, G. J. (2015). pH Effects on solubility, zeta potential, and correlation between antibacterial activity and molecular weight of chitosan. *Carbohydrate Polymers, 134*, 74–81.

Cruz-Romero, M. C., Murphy, T., Morris, M., Cummins, E., & Kerry, J. P. (2013). Antimicrobial activity of chitosan, organic acids and nano-sized solubilisates for potential use in smart antimicrobially-active packaging for potential food applications. *Food Control, 34*(2), 393–397.

De Lima, R., Feitosa, L., Pereira, A. D. E. S., De. Moura, M. R., Aouada, F. A., et al. (2010). Evaluation of the genotoxicity of chitosan nanoparticles for use in food packaging films. *Journal of Food Science, 75*(6).

Du, W. L., Niu, S. S., Xu, Y. L., Xu, Z. R., & Fan, C. L. (2009). Antibacterial activity of chitosan tripolyphosphate nanoparticles loaded with various metal ions. *Carbohydrate Polymers, 75*(3), 385–389.

Fan, W., Yan, W., Xu, Z., & Ni, H. (2012). Formation mechanism of monodisperse, low molecular weight chitosan nanoparticles by ionic gelation technique. *Colloids and Surfaces B: Biointerfaces, 90*, 21–27.

Fàbregas, A., Miñarro, M., García-Montoya, E., Pérez-Lozano, P., Carrillo, C., Sarrate, R., Sánchez, N., Ticó, J. R., & Suñé-Negre, J. M. (2013). Impact of physical parameters on particle size and reaction yield when using the ionic gelation method to obtain cationic polymeric chitosan–tripolyphosphate nanoparticles. *International Journal of Pharmaceutics, 446*(1), 199–204.

Feyzioglu, G. C., & Tornuk, F. (2016). Development of chitosan nanoparticles loaded with summer savory (Satureja hortensis L.) essential oil for antimicrobial and antioxidant delivery applications. *Lebensmittel-Wissenschaft und -Technologie-Food Science and Technology, 70*, 104–110.

Mi, F., Shyu, S., Lee, S., & Wong, T. (1999). Kinetic study of chitosan-tripolyphosphate complex reaction and acid-resistive properties of the chitosan-tripolyphosphate gel beads prepared by in-liquid curing method. *Journal of Polymer Science Part B: Polymer Physics, 37*(14), 1551–1564.

Gamboa, A., Araujo, V., Caro, N., Gotteland, M., Abugoch, L., & Tapia, C. (2015). Spray freeze-drying as an alternative to the ionic gelation method to produce chitosan and alginate nano-particles targeted to the colon. *Journal of Pharmaceutical Sciences, 104*(12), 4373–4385.

Gokce, Y., Cengiz, B., Yildiz, N., Calimli, A., & Aktas, Z. (2014). Ultrasonication of chitosan nanoparticle suspension: Influence on particle size. *Colloids and Surfaces a: Physicochemical and Engineering Aspects, 462*, 75–81.

Goy, R. C., Morais, S. T. B., & Assis, O. B. G. (2016). Evaluation of the antimicrobial activity of chitosan and its quaternized derivative on E. coli and S. aureus growth. *Revista Brasileira de Farmacognosia, 26*(1), 122–127.

Hosseini, S. F., Rezaei, M., Zandi, M., & Farahmandghavi, F. (2016). Preparation and characterization of chitosan nanoparticles-loaded fish gelatin-based edible films. *Journal of Food Process Engineering, 39*(5), 521–530.

Hu, J., Wang, X. G., Xiao, Z. B., & Bi, W. C. (2015). Effect of chitosan nanoparticles loaded with cinnamon essential oil on the quality of chilled pork. *Lebensmittel-Wissenschaft und -Technologie- Food Science and Technology, 63*(1), 519–526.

Kafshgari, M. H., Khorram, M., Mansouri, M., Samimi, A., & Osfouri, S. (2012). Preparation of alginate and chitosan nanoparticles using a new reverse micellar system. *Iranian Polymer Journal (English Edition), 21*(2), 99–107.

Kheiri, A., Moosawi Jorf, S. A., Malihipour, A., Saremi, H., & Nikkhah, M. (2016). Application of chitosan and chitosan nanoparticles for the control of Fusarium head blight of wheat (Fusarium graminearum) in vitro and greenhouse. *International Journal of Biological Macromolecules, 93*(Part A), 1261–1272.

Kong, M., Chen, X. G., Xing, K., & Park, H. J. (2010). Antimicrobial properties of chitosan and mode of action: A state of the art review. *International Journal of Biological Macromolecules, 144*(1), 51–63.

Liu, N., Chen, X. G., Park, H. J., Liu, C. G., Liu, C. S., Meng, X. H., et al. (2006). Effect of MW and concentration of chitosan on antibacterial activity of Escherichia coli. *Carbohydrate Polymers, 64*(1), 60–65.

Li, J., Wu, Y., & Zhao, L. (2016). Antibacterial activity and mechanism of chitosan with ultra high molecular weight. *Carbohydrate Polymers, 148*, 200–205.

Madureira, A. R., Pereira, A., Castro, P. M., & Pintado, M. (2015). Production of antimicrobial chitosan nanoparticles against food pathogens. *Journal of Food Engineering, 167*, 210–216.

Maillard, J. Y., & Hartemann, P. (2013). Silver as an antimicrobial: Facts and gaps in knowledge. *Critical Reviews in Microbiology, 39*(4), 373–383.

Ma, Y., Liu, P., Si, C., & Liu, Z. (2010). Chitosan Nanoparticles: Preparation and application in antibacterial paper. *Journal of Macromolecular Science, Part B, 49*(5), 994–1001.

Mohanraj, V. J., & C, Y. (2006). Nanoparticles - a review. *Journal of Pharmaceutical Research, 5*(1), 561–573.

de Moura, M. R., Aouada, F. A., & Mattoso, L. H. C. (2008). Preparation of chitosan

nanoparticles using methacrylic acid. *Journal of Colloid and Interface Science, 321*(2), 477–483.
NCCLS. (2000). *Methods for dilution antimicrobial susceptibility tests for bacteria that grow aerobically—Fifth edition: Approved standard M7–A5* (NCCLS, Ed.). Wayne, PA, USA.
Ngan, L. T. K., Wang, S. L., Hiep, D. M., Luong, P. M., Vui, N. T., Dinh, T. M., et al. (2014). Preparation of chitosan nanoparticles by spray drying, and their antibacterial activity. *Research on Chemical Intermediates, 40*(6), 2165–2175.
O'Callaghan, K. A. M., & Kerry, J. P. (2016). Preparation of low- and medium-molecular weight chitosan nanoparticles and their antimicrobial evaluation against a panel of microorganisms, including cheese-derived cultures. *Food Control, 69*, 256–261.
Paomephan, P., Assavanig, A., Chaturongakul, S., Cady, N. C., Bergkvist, M., & Niamsiri, N. (2018). Insight into the antibacterial property of chitosan nanoparticles against Escherichia coli and Salmonella Typhimurium and their application as vegetable wash disinfectant. *Food Control, 86*, 294–301.
Park, S. I., Marsh, K. S., & Dawson, P. (2010). Application of chitosan-incorporated LDPE film to sliced fresh red meats for shelf life extension. *Meat Science, 85*(3), 493–499.
Pilon, L., Spricigo, P. C., Miranda, M., de Moura, M. R., Assis, O. B. G., et al. (2015). Chitosan nanoparticle coatings reduce microbial growth on fresh-cut apples while not affecting quality attributes. *International Journal of Food Science and Technology, 50*(2), 440–448.
de Pinho Neves, A. L., Milioli, C. C., Müller, L., Riella, H. G., Kuhnen, N. C., & Stulzer, H. K. (2014). Factorial design as tool in chitosan nanoparticles development by ionic gelation technique. *Colloids and Surfaces a: Physicochemical and Engineering Aspects, 445*, 34–39.
Qi, L., Xu, Z., Jiang, X., Hu, C., & Zou, X. (2004). Preparation and antibacterial activity of chitosan nanoparticles. *Carbohydrate Research, 339*(16), 2693–2700.
Qun, G., & Ajun, W. (2006). Effects of molecular weight, degree of acetylation and ionic strength on surface tension of chitosan in dilute solution. *Carbohydrate Polymers, 64*(1), 29–36.
Rabea, E. I., Badawy, M. E., Stevens, C. V., Smagghe, G., & Steurbaut, W. (2003). Chitosan as antimicrobial agent: Applications and mode of action. *Biomacromolecules, 4*(6), 1457–1465.
Rathi, N., & Gaikar, V. G. (2017). Optimization of continuous synthesis of cross-linked chitosan nanoparticles using microreactors. *Chemical Engineering & Technology, 40*(3), 506–513.
Czechowska-Biskup, R., Rokita, B., Lotfy, S., Ulanski, P., & Rosiak, J. M. (2005). Degradation of chitosan and starch by 360-kHz ultrasound. *Carbohydrate Polymers, 60*(2), 175–184.
Ristić, T., Lasič, S., Kosalec, I., Bračič, M., & Fras-Zemljič, L. (2015). The effect of chitosan nanoparticles onto Lactobacillus cells. *Reactive and Functional Polymers, 97*, 56–62.
Ryan, C. C., Delezuk, J. A. M., Pavinatto, A., Oliveira, O. N., Fudouzi, H., Pemble, M. E., et al. (2016). Silica-based photonic crystals embedded in a chitosan-TEOS matrix: Preparation, properties and proposed applications. *Journal of Materials Science, 51*(11), 5388–5396.
Sanguansri, P., & Augustin, M. A. (2006). Nanoscale materials development—a food industry perspective. *Trends in Food Science & Technology, 17*(10), 547–556.
Shahbazi, M., Rajabzadeh, G., & Ahmadi, S. J. (2017). Characterization of nanocomposite film based on chitosan intercalated in clay platelets by electron beam irradiation. *Carbohydrate Polymers, 157*, 226–235.
Simon-Deckers, A., Loo, S., Mayne-L'hermite, M., Herlin-Boime, N., Menguy, N., Reynaud, C., et al. (2009). Size-, composition- and shape-dependent toxicological impact of metal oxide nanoparticles and carbon nanotubes toward bacteria. *Environmental Science & Technology, 43*(21), 8423–8429.
Souza, H. K. S., Campiña, J. M., Sousa, A. M. M., Silva, F., & Gonçalves, M. P. (2013). Ultrasound-assisted preparation of size-controlled chitosan nanoparticles: Characterization and fabrication of transparent biofilms. *Food Hydrocolloids, 31*(2), 227–236.
Sullivan, D. J., Azlin-Hasim, S., Cruz-Romero, M., Cummins, E., Kerry, J. P., & Morris, M. A. (2018). 11-Natural antimicrobial materials for use in food packaging a2-tiwari, atul. In *Handbook of antimicrobial coatings* (pp. 181–233). Elsevier.
Tran, H. V., Tran, L. D., Ba, C. T., Vu, H. D., Nguyen, T. N., Pham, D. G., et al. (2010). Synthesis, characterization, antibacterial and antiproliferative activities of monodisperse chitosan- based silver nanoparticles. *Colloids and Surfaces a: Physicochemical and Engineering Aspects, 360*(1–3), 32–40.
Wang, Y. B., Liu, L., Zhou, J. R., Ruan, X. M., Lin, J. D., & Fu, L. L. (2015). Effect of chitosan nanoparticle coatings on the quality changes of postharvest whiteleg shrimp, Litopenaeus vannamei, during storage at 4 °C. *Food and Bioprocess Technology, 8*(4), 907–915.
Wang, Y., Zhou, J., Liu, L., Huang, C., Zhou, D., & Fu, L. (2016). Characterization and toxicology evaluation of chitosan nanoparticles on the embryonic development of zebrafish, Danio rerio. *Carbohydrate Polymers, 141*, 204–210.
Wu, T., Zivanovic, S., Hayes, D. G., & Weiss, J. (2008). Efficient reduction of chitosan molecular weight by high-intensity ultrasound: Underlying mechanism and effect of process parameters. *Journal of Agricultural and Food Chemistry, 56*(13), 5112–5119.
Zain, N. M., Stapley, A. G., & Shama, G. (2014). Green synthesis of silver and copper nanoparticles using ascorbic acid and chitosan for antimicrobial applications. *Carbohydrate Polymers, 112*, 195–202.
Zarei, M., Ramezani, Z., Ein-Tavasoly, S., & Chadorbaf, M. (2015). Coating effects of orange and pomegranate peel extracts combined with chitosan nanoparticles on the quality of refrigerated silver carp fillets. *Journal of Food Processing and Preservation, 39*(6), 2180–2187.
Zhang, W., Zhang, J. L., & Xia, W. S. (2012). The preparation of chitosan nanoparticles by wet media milling. *International Journal of Food Science and Technology, 47*(11), 2266–2272.